Improved measurement accuracy in optical scatterometry using correction-based library search

Xiuguo Chen,[1] Shiyuan Liu,[1,2,*] Chuanwei Zhang,[2] and Hao Jiang[3]

[1]Wuhan National Laboratory for Optoelectronics, Huazhong University of Science and Technology, Wuhan, Hubei 430074, China

[2]State Key Laboratory of Digital Manufacturing Equipment and Technology, Huazhong University of Science and Technology, Wuhan, Hubei 430074, China

[3]Department of Mechanical and Aerospace Engineering, University of Texas at Arlington, Arlington, Texas 76019, USA

*Corresponding author: shyliu@mail.hust.edu.cn

Received 7 March 2013; revised 20 August 2013; accepted 22 August 2013; posted 23 August 2013 (Doc. ID 186568); published 16 September 2013

Library search is one of the most commonly used methods for solving the inverse problem in optical scatterometry. The final measurement accuracy of the conventional library search method highly depends on the grid interval selected for each parameter in the signature library, and the time cost of the parameter extraction increases dramatically when the grid interval is decreasing. In this paper, we propose a correction-based library search method to improve the measurement accuracy for a pregenerated signature library. We derive a formulation to estimate the error between the expected solution of the inverse problem and the actually searched solution obtained by the conventional library search method. Then we use the estimate of the error as a correction term to correct the actually searched solution to improve the measurement accuracy. Experiments performed on a photoresist grating have demonstrated that the proposed correction-based library search method can achieve much more accurate measurement with negligible computational penalty to the conventional library search method in the parameter extraction. It has also been observed that the correction-based library search method has higher measurement accuracy and less time cost than the interpolation-based library search method. The proposed correction-based library search method is expected to provide a more practical means to solve the inverse problem in state-of-the-art optical scatterometry.

OCIS codes: (120.0120) Instrumentation, measurement, and metrology; (290.3200) Inverse scattering; (050.1950) Diffraction gratings; (120.2130) Ellipsometry and polarimetry.

http://dx.doi.org/10.1364/AO.52.006726

1. Introduction

Process control in microelectronic manufacturing requires real-time monitoring techniques. Among the different techniques, optical scatterometry, sometimes referred to as optical critical dimension (OCD) metrology, has recently achieved great success in the monitoring of CD and overlay [1–6]. There are two main procedures in optical scatterometry. The first involves the calculation of the theoretical signature from a diffractive structure using reliable forward-modeling techniques, such as the rigorous coupled-wave analysis (RCWA) [7–9], the finite element method (FEM) [10,11], the boundary element method (BEM) [12], or the finite-difference time-domain (FDTD) method [13]. Here the general term signature contains the scattered light information from the diffractive structure, which can be in the form of reflectance, ellipsometric angles, Stokes

1559-128X/13/276726-09$15.00/0

vector elements, or Mueller matrix elements. The second procedure involves the reconstruction of the structural profile from the measured signature, which is a typical inverse problem with the objective of finding a profile whose theoretical signature can best match the measured one.

To solve the inverse problem in optical scatterometry, several methods have been reported in recent years. Drége *et al.* presented a linearized method to obtain surface profile information by the linearized inversion of scatterometric data [14]. The linearized method has its inherent limitation due to the highly nonlinear relationship between the optical signature and the profile parameters. Some nonlinear regression techniques, such as the Levenberg–Marquardt (LM) algorithm and its improved technique by combining with the artificial neural network (ANN) [15], have also been proposed. Although the nonlinear regression techniques can achieve the expected solution of the inverse problem if there is convergence, they are usually time-consuming because the expected solution is achieved through an iterative procedure that repeatedly requires computation of the forward optical modeling. This is even worse and unacceptable when dealing with two-dimensional or more complex structures. A feasible way to meet the *in situ* requirement, known as library search, is to generate a signature library prior to the measurement and then to search in the library to find a best match with the measured signature [16,17]. Although the offline generation of the signature library is time-consuming, the search itself during the online measurement can be done quickly with a global solution guaranteed [18]. Therefore the library search method has been demonstrated to be an effective approach to solve the inverse problem in optical scatterometry and has been commonly used in industry [19,20].

The success of a library search relies heavily on two essential aspects: the signature library and the search algorithm. In the past decades, several library search algorithms such as the linear search, k-dimensional tree search, and locality-sensitive hashing have been reported with an emphasis on matching accurately and rapidly [21–23]. Besides the library search algorithm itself, the scale of the signature library is closely related to the final measurement accuracy and the speed of library search. The scale of a signature library is determined by the ranges of structural parameters and the associated grid interval selected for each parameter. The ranges of structural parameters, typically depending on the process tolerances, are usually specified at $\pm 10\%$ of their nominal dimensions as a rule of thumb [16]. One issue in the conventional library search method is that its measurement accuracy is fundamentally limited by the grid interval. In general, the measurement accuracy of library search can be improved by decreasing the grid interval. However, it will take much more time and memory space to generate and store the signatures, and a too large signature library will also greatly influence the speed of library search. Some efforts have been made to deal with this issue. Ku *et al.* presented a feature region algorithm based on sensitivity analysis to reduce the scale of the signature library [24]. Littau *et al.* investigated several techniques to determine an optimal signature scan path that can also result in a smaller signature library [25]. In our recent work, a fitting error interpolation-based library search method was reported to improve the measurement accuracy for a pregenerated library [26].

In this paper, we propose a correction-based library search method to improve the measurement accuracy for a pregenerated signature library. As the solution of the inverse problem obtained by the conventional library search method is directly searched among the grid points in the library, there will be a deterministic error between the expected solution of the inverse problem and the actually searched solution obtained by the conventional library search method due to the limitation of the grid interval. We derive a formulation to estimate the error based on the linear model of the theoretical signature of the diffractive structure. Then we use the estimate of the error as a correction term to correct the actually searched solution. The corrected solution will be much closer to the expected solution and therefore improves the final measurement accuracy. The key in the correction-based library search method is the estimation of the error, which can be conducted by using the theoretical signatures prestored in the library. Hence, the time-consuming forward modeling is completely avoided in the correction-based library search method. It is therefore also expected that the estimation of the error in the proposed correction-based library search method will have no remarkable influence on its time cost in the parameter extraction.

The remainder of this paper is organized as follows. Section 2 first briefly introduces the inverse problem in optical scatterometry and then presents the correction-based library search method in detail. Section 3 provides the experimental results to demonstrate the higher accuracy and fast search ability of the proposed method in comparison with the conventional library search as well as the interpolation-based library search. Finally, we draw some conclusions in Section 4.

2. Method

A. Inverse Problem in Optical Scatterometry

Without loss of generality, we denote the structural parameters under measurement as an M-dimensional vector $\mathbf{x} = [x_1, x_2, \ldots, x_M]^{\mathrm{T}}$, where the superscript "T" represents the transpose and $x_1, x_2, \ldots, x_M$ can be the linewidth, line height, and sidewall angle of the grating sample. The measured signature is given by an N-dimensional vector $\mathbf{y} = [y_1, y_2, \ldots, y_N]^{\mathrm{T}}$, and the corresponding theoretical signature associated with $\mathbf{x}$ is given by $\mathbf{f}(\mathbf{x}) = [f_1(\mathbf{x}), f_2(\mathbf{x}), \ldots, f_N(\mathbf{x})]^{\mathrm{T}}$. The χ^2

function is usually applied to estimate the fitting error between measured and theoretical signatures, which is defined by

$$\chi^2 = \sum_{i=1}^{N} w_i[y_i - f_i(\mathbf{x})]^2, \tag{1}$$

where the w_i are the weighting factors. Usually, if the variances $\sigma^2(y_i)$ are known, the weighting factors are chosen to be $w_i = 1/\sigma^2(y_i)$. Equation (1) can be written as a matrix expression with a format similar to Eq. (2) as presented in Ref. [27]

$$\chi^2 = [\mathbf{y} - \mathbf{f}(\mathbf{x})]^{\mathrm{T}}\mathbf{W}[\mathbf{y} - \mathbf{f}(\mathbf{x})], \tag{2}$$

where $\mathbf{W}$ is an $N \times N$ diagonal matrix with diagonal elements w_i. The inverse problem in optical scatterometry is typically formulated as a least squares regression problem such that

$$\hat{\mathbf{x}} = \arg\min_{\mathbf{x}\in\Omega}\{[\mathbf{y} - \mathbf{f}(\mathbf{x})]^{\mathrm{T}}\mathbf{W}[\mathbf{y} - \mathbf{f}(\mathbf{x})]\}, \tag{3}$$

where $\hat{\mathbf{x}}$ is the solution of the inverse problem that contains the extracted structural parameters, and Ω is the associated parameter domain.

B. Correction-Based Library Search

The above inverse problem can be solved by applying different approaches. For convenience, $\mathbf{x}_e$ is assumed to be an estimate of the true value of $\mathbf{x}$ in a continuous space of solutions of the inverse problem, which minimizes Eq. (2) and satisfies

$$\chi^2_{\min} = [\mathbf{y} - \mathbf{f}(\mathbf{x}_e)]^{\mathrm{T}}\mathbf{W}[\mathbf{y} - \mathbf{f}(\mathbf{x}_e)]. \tag{4}$$

It is noted that $\mathbf{x}_e$ is also the expected solution of the inverse problem that we attempt to find. We will not discuss the various approaches used to achieve the expected solution $\mathbf{x}_e$; what we need to know is that such a solution exists in reality. We assume that the actually searched solution obtained by conventional library search method is denoted as $\mathbf{x}_s$, which corresponds to the discrete grid point in the pregenerated signature library whose theoretical signature can best match the measured one. Obviously, $\mathbf{x}_s$ is also an estimate of the true value of $\mathbf{x}$, but is in a discrete space of solutions of the inverse problem. In addition, the searched solution $\mathbf{x}_s$ is close to the expected solution $\mathbf{x}_e$. However, due to the limitation of the grid interval of the library, there will be a deterministic error $\Delta\mathbf{x}$ between the solutions $\mathbf{x}_s$ and $\mathbf{x}_e$, which is defined by

$$\Delta\mathbf{x} = \mathbf{x}_e - \mathbf{x}_s. \tag{5}$$

We assume that the function $\mathbf{f}(\mathbf{x})$ is sufficiently smooth and can be expanded in a Taylor series, which, truncated to the first order, leads to a linear model at $\mathbf{x} = \mathbf{x}_s$:

$$\mathbf{f}(\mathbf{x}) = \mathbf{f}(\mathbf{x}_s) + \mathbf{J}\cdot(\mathbf{x} - \mathbf{x}_s), \tag{6}$$

where $\mathbf{J}$ is the $N \times M$ Jacobian matrix with respect to $\mathbf{x}$, whose elements are given by

$$[\mathbf{J}]_{ij} = \left.\frac{\partial f_i(\mathbf{x})}{\partial x_j}\right|_{\mathbf{x}=\mathbf{x}_s}. \tag{7}$$

Let $\mathbf{x} = \mathbf{x}_e$ in Eq. (6), we have

$$\mathbf{f}(\mathbf{x}_e) = \mathbf{f}(\mathbf{x}_s) + \mathbf{J}\cdot(\mathbf{x}_e - \mathbf{x}_s) = \mathbf{f}(\mathbf{x}_s) + \mathbf{J}\Delta\mathbf{x}. \tag{8}$$

Inserting Eq. (8) into Eq. (4), we have

$$\chi^2_{\min} = [\mathbf{y} - \mathbf{f}(\mathbf{x}_s) - \mathbf{J}\Delta\mathbf{x}]^{\mathrm{T}}\mathbf{W}[\mathbf{y} - \mathbf{f}(\mathbf{x}_s) - \mathbf{J}\Delta\mathbf{x}]. \tag{9}$$

By taking the derivative of both sides of Eq. (9) with respect to $\mathbf{x}$, we can derive that

$$\tilde{\mathbf{J}}\Delta\mathbf{x} = \mathbf{W}^{1/2}[\mathbf{y} - \mathbf{f}(\mathbf{x}_s)], \tag{10}$$

where $\tilde{\mathbf{J}} = \mathbf{W}^{1/2}\mathbf{J}$ is called the weighted Jacobian matrix. According to Eq. (10), we have

$$\Delta\mathbf{x} = \tilde{\mathbf{J}}^{+}\mathbf{W}^{1/2}[\mathbf{y} - \mathbf{f}(\mathbf{x}_s)], \tag{11}$$

where $\tilde{\mathbf{J}}^{+}$ is the Moore–Penrose pseudo-inverse of matrix $\tilde{\mathbf{J}}$, and $\tilde{\mathbf{J}}^{+} = (\tilde{\mathbf{J}}^{\mathrm{T}}\tilde{\mathbf{J}})^{-1}\tilde{\mathbf{J}}^{\mathrm{T}}$. Equation (11) gives the estimate of the error $\Delta\mathbf{x}$ between the solutions $\mathbf{x}_s$ and $\mathbf{x}_e$. It is noted that a similar formula to Eq. (11) is also presented in Ref. [28] but is derived in a different approach. We can further use the estimate of the error $\Delta\mathbf{x}$ given by Eq. (11) as a correction term to correct the searched solution $\mathbf{x}_s$ and derive that

$$\mathbf{x}_c = \mathbf{x}_s + \tilde{\mathbf{J}}^{+}\mathbf{W}^{1/2}[\mathbf{y} - \mathbf{f}(\mathbf{x}_s)], \tag{12}$$

where $\mathbf{x}_c$ denotes the corrected solution of the inverse problem. Figure 1 presents a geometrical illustration of the corrected solution $\mathbf{x}_c$ given by Eq. (12). As shown in Fig. 1, the curve around point B can be approximated by a straight line with slope $\tilde{\mathbf{J}}$ at $\mathbf{x} = \mathbf{x}_s$. The term $\mathbf{W}^{1/2}[\mathbf{y} - \mathbf{f}(\mathbf{x}_s)]$ in Eq. (11) denotes the residual signature between the points A and B. According to the slope $\tilde{\mathbf{J}}$ as well as the residual signature $\mathbf{W}^{1/2}[\mathbf{y} - \mathbf{f}(\mathbf{x}_s)]$, we can derive the corrected solution $\mathbf{x}_c$ given by Eq. (12). As depicted in Fig. 1, the corrected solution $\mathbf{x}_c$ will be much closer to the expected solution $\mathbf{x}_e$ than the searched solution $\mathbf{x}_s$ and therefore improves the accuracy of the solution of the inverse problem.

According to Eq. (12), we propose a correction-based library search method to improve the measurement accuracy for a pregenerated signature library. The basic procedure of the correction-based library search is described as follows.

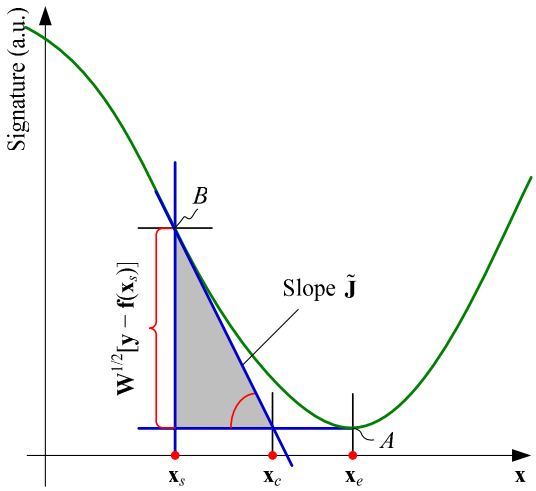

Fig. 1. Geometrical illustration of the corrected solution $\mathbf{x}_c$ to the inverse problem in optical scatterometry.

Step 1: Obtain the searched solution $\mathbf{x}_s$ of the inverse problem in optical scatterometry as described in Eq. (3) by the conventional library search method.

Step 2: Calculate the estimate of the error $\Delta\mathbf{x}$ between the searched solution $\mathbf{x}_s$ and the expected solution $\mathbf{x}_e$ according to Eq. (11).

Step 3: Correct the searched solution $\mathbf{x}_s$ by using the estimate of the error $\Delta\mathbf{x}$ according to Eq. (12) and take the corrected solution $\mathbf{x}_c$ as the final measurement result.

The key in the correction-based library search method is the estimation of the error $\Delta\mathbf{x}$ given by Eq. (11), which involves the calculation of the Jacobian matrix $\mathbf{J}$ as well as the pseudo-inverse of the weighted Jacobian matrix $\tilde{\mathbf{J}}^{+}$. The elements of matrix $\mathbf{J}$, which are given by Eq. (7), are estimated in the correction-based library search method by

$$\left.\frac{\partial f_i(\mathbf{x})}{\partial x_j}\right|_{\mathbf{x}=\mathbf{x}_s} = \frac{f_i(\mathbf{x}_s+\delta_j\mathbf{e}_j)-f_i(\mathbf{x}_s-\delta_j\mathbf{e}_j)}{2\delta_j}+O(\delta_j^2), \quad (13)$$

where $\mathbf{e}_j$ is the unit vector in the j-th coordinate direction and δ_j is the grid interval of the j-th structural parameter in the library. The theoretical signatures $\mathbf{f}(\mathbf{x}_s+\delta_j\mathbf{e}_j)$ and $\mathbf{f}(\mathbf{x}_s-\delta_j\mathbf{e}_j)$ in Eq. (13) can be directly searched among the grid points in the pregenerated signature library, thus the time-consuming forward modeling is avoided in the estimation of the error $\Delta\mathbf{x}$. The only extra time cost in the correction-based library search method is introduced by the matrix multiplication, which is ignorable. Therefore the proposed correction-based library search method is expected to achieve more accurate measurement for a pregenerated signature library without remarkable influence on the final search speed.

3. Results

A. Measurement Setup

The scatterometric measurement was conducted on a dual-rotating compensator ellipsometer (RC2 ellipsometer, J. A. Woollam Co.) with in-house forward-modeling software based on RCWA [7–9]. As schematically shown in Fig. 2, the system configuration of the RC2 ellipsometer in order of light propagation is $PC_{r1}SC_{r2}A$, where P and A stand for the fixed polarizer and analyzer, C_{r1} and C_{r2} refer to the first and second frequency-coupled rotating compensators, and S stands for the sample. With the light source used in this ellipsometer, the wavelengths available are in the 193–1690 nm range, covering the spectral range of 250–800 nm used in this paper. The incidence angle is fixed at 65°, and the plane of incidence is perpendicular to the grating lines with the azimuthal angle equal to 0° in the process of data collection.

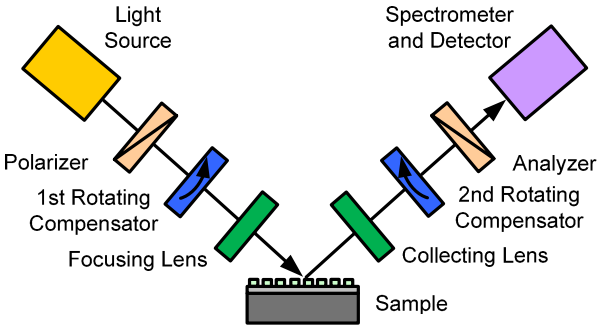

Fig. 2. Scheme of the dual-rotating compensator ellipsometer.

As shown in Fig. 3, the investigated sample is a silicon wafer that contains 35 dies, and each die consists of a photoresist grating array on a bottom antireflective coating (BARC) layer deposited on the silicon substrate. The profile of the grating structure is characterized by top critical dimension *TCD*, sidewall angle *SWA*, grating height Hgt_1, and period *pitch*. The thickness of the BARC layer is denoted as Hgt_2. Nominal dimensions of the grating structure are $TCD = 200$ nm; $SWA = 90°$; $Hgt_1 = 311$ nm; $pitch = 400$ nm; and $Hgt_2 = 115$ nm. Optical properties of the BARC layer were determined in advance before the photoresist layer was coated on it. Optical properties of silicon substrate were taken from Ref. [29]. In the selected spectral range of 250–800 nm, optical properties of the photoresist layer were modeled by the Tauc–Lorentz model [30] with the nondispersive term $\varepsilon_\infty = 1.3205$, the

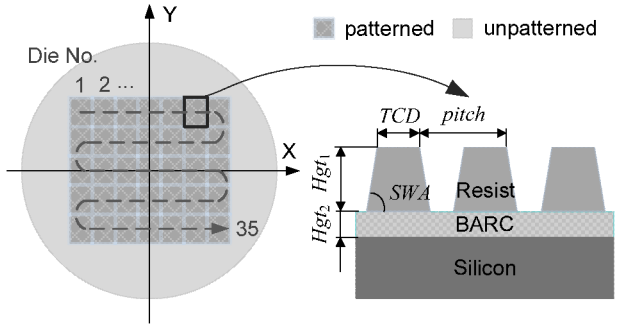

Fig. 3. Schematic diagram of the silicon wafer and the photoresist grating structure.

Tauc gap energy $E_g = 3.9572$ eV, the amplitude $A_{TL} = 29.6462$ eV, the broadening parameter $C_{TL} = 1.4317$ eV, and the Lorentz resonant frequency $E_0 = 10.0527$ eV. In the experiments, structural parameters of the investigated sample that need to be extracted include *TCD*, Hgt_1, and *SWA*, while the grating period *pitch* and thickness of the BARC layer Hgt_2 are fixed at their nominal dimensions.

Two signature libraries with different grid intervals for the investigated grating structure were constructed prior to the measurements. Details of the constructed signature libraries are listed in Table 1. The optical signatures of the grating structure stored in the library are in the forms of Stokes vector elements, which are defined by $S_1 = \cos 2\psi$, $S_2 = \sin 2\psi \cos \Delta$, and $S_3 = \sin 2\psi \sin \Delta$. Here, ψ and Δ are the ellipsometric angles. The theoretical signatures of the grating structure are calculated in the spectral range of 250–800 nm with an increment of 2 nm, and in the incidence and azimuthal angles 65° and 0°, respectively. The number of retained orders in the truncated Fourier series when applying RCWA to calculate the theoretical signatures is 12. The grating structure is sliced into 15 layers along the vertical direction in the calculation.

B. Experimental Results

The photoresist grating structure was measured die by die by using the RC2 ellipsometer in order to demonstrate the validity of the proposed correction-based library search method. We assess the accuracy of the solution of the inverse problem as described in Eq. (3) by

$$\boldsymbol{\varepsilon}_l = |\hat{\mathbf{x}}^{(l)} - \mathbf{x}_0^{(l)}|, \qquad \bar{\boldsymbol{\varepsilon}} = \frac{1}{L}\sum_{l=1}^{L} \boldsymbol{\varepsilon}_l, \tag{14}$$

where $\boldsymbol{\varepsilon}_l$ represents the absolute error for the l-th test, $\bar{\boldsymbol{\varepsilon}}$ is the mean absolute error for the total number of L tests, $\hat{\mathbf{x}}^{(l)}$ is the vector that consists of the extracted structural parameters for the l-th test, and $\mathbf{x}_0^{(l)}$ is the vector that consists of the corresponding reference parameter values for the l-th test. In the experiments, since the true structural parameter values associated with the measured signatures are unknown, we used the structural parameters extracted by the LM algorithm as the reference parameter values to assess the solution accuracy. The LM algorithm can achieve accurate results if suitable initial values are provided. In our previous work, an ANN and LM combined method was proposed for solving the inverse problem in reflectometry [15]. In the ANN-LM combined method, an initial estimate of the structural parameters is quickly generated from the measured signature by the ANN, and then the accurate result is further obtained by the LM algorithm. It has been demonstrated that the combined parameter extraction method can achieve improved performance over the ANN or LM algorithm alone and can lead to highly accurate measurement results. In our experiments, we first used the pregenerated signature library (Library 1#), as depicted in Table 1, as a training set to train a back-propagation neural network, and then input the measured signatures into the trained network. The mapping results of the neural network were then selected as the initial values of the LM algorithm for further parameter extraction. Finally, 35 dies of the grating sample shown in Fig. 3 were measured by using the critical dimension scanning electron microscope (CD-SEM S-9200, Hitachi), of which two dies were measured by using the cross-section SEM (Nova NanoSEM450, FEI). We compared the structural parameters extracted by the ANN-LM combined method with those measured by SEM, and good agreements have been observed. It is worth pointing out that the validity of taking the measurement result of the ANN-LM combined method as the reference has been also demonstrated in our recent work [26].

We first applied the conventional library search method, the proposed correction-based library search method as well as the interpolation-based library search method to extract structural parameters from the measured signatures with Library 1#. In the applied interpolation-based library search method, the fitting error between the measured signature and any theoretical signature that is not prestored in the library is estimated by interpolating on the known fitting errors associated with the discrete grid points [26]. By comparing the interpolated fitting errors, the structural parameters corresponding to the minimum interpolated fitting error are treated as the final measurement result. Figure 4 depicts the absolute errors of the extracted structural parameters *TCD*, Hgt_1, and *SWA* for each die of the silicon wafer. The mean absolute error associated with each structural parameter is shown in the bottom right corner of Fig. 4. It is observed from Fig. 4 that the final measurement accuracy is indeed dramatically improved by using the correction-based library search method and the interpolation-based library

Table 1. Details of the Signature Libraries Used in the Experiments

	Library 1#			Library 2#		
Parameter Name	Parameter Range	Grid Interval	Library Scale (No. of Signatures)	Parameter Range	Grid Interval	Library Scale (No. of Signatures)
TCD	160–210 nm	1 nm	$51 \times 26 \times 26 = 34,476$	160–210 nm	3 nm	$20 \times 9 \times 13 = 2340$
Hgt_1	290–315 nm	1 nm		290–315 nm	3 nm	
SWA	85°–90°	0.2°		85°–90°	0.4°	

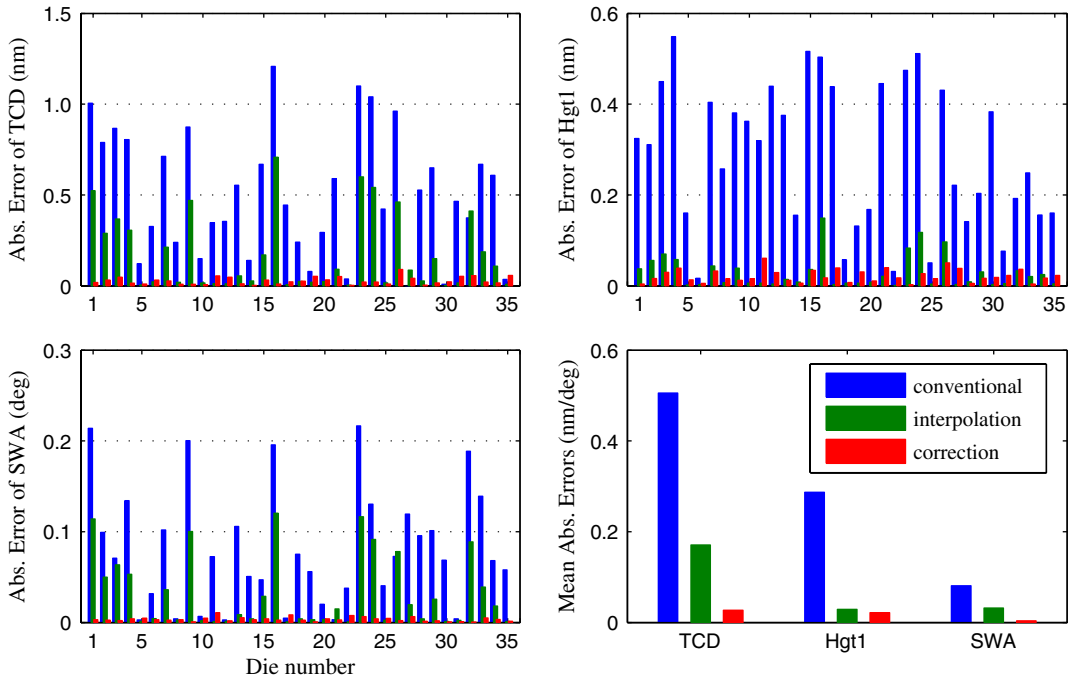

Fig. 4. Absolute errors of the structural parameters *TCD*, Hgt_1, and *SWA* obtained with Library 1# by the conventional library search method, the interpolation-based library search method, and the correction-based library search method. The mean absolute errors of the extracted structural parameters for the 35 dies of the investigated silicon wafer are shown in the bottom right corner.

search method. Moreover, the measurement accuracy of the correction-based library search method is also much higher than that of the interpolation-based library search method. For example, Table 2 presents the extracted structural parameters for the No. 16 die of the grating sample shown in Fig. 3. The last column of Table 2 gives the root-mean-square error (RMSE) between the measured and the corresponding calculated Stokes vector elements. Figure 5 depicts the measured Stokes vector elements and the fitted Stokes vector elements calculated from the structural parameters presented in Table 2 extracted by the conventional library search method, the interpolation-based library search method, the correction-based library search method, and the ANN-LM combined method, respectively. As shown in Fig. 5(a), the measured and calculated Stokes vector elements exhibit good agreement over most of the spectrum except the range from about 750 to 780 nm, where there exists a cusp in the third calculated Stokes vector element S_3. It was found in our experiments that the cusp was attributed to the depolarization effect induced by the finite numerical aperture (NA) of the focusing lens in the RC2 ellipsometer. We also found that there was an offset of about 2.8° in the azimuthal angle. The depolarization effect induced by the NA and the offset in the azimuthal angle were demonstrated to induce fitting errors between the measured and calculated Stokes vector elements while having negligible impacts on the final extracted structural parameters. In addition, although it is not so obvious in Fig. 5(a), it indeed can be observed from Fig. 5(b) and Table 2 that the ANN-LM combined method achieves the lowest fitting error, the proposed correction-based library search method almost has the same fitting performance to the ANN-LM combined method, and both of them outperform the interpolation-based library search method and the conventional library search method. This experimental observation confirms again that more accurate measurement can be achieved for a pregenerated signature library by applying the proposed correction-based library search method.

Table 2. Comparison of the Structural Parameters Extracted by the Conventional Library Search Method, the Interpolation-Based Library Search Method, the Correction-Based Library Search Method, and the ANN-LM Combined Method

Algorithm	*TCD* (nm)	Hgt_1 (nm)	*SWA* (degree)	RMSE
Conventional	164	299	88.8	1.84756
Interpolation	164.500	298.645	88.875	1.84220
Correction	165.198	298.514	88.998	1.84075
ANN-LM	165.208	298.496	88.996	1.84074

The time cost of the conventional library search method, the interpolation-based library search method, and the correction-based library search method in the parameter extraction with Library 1# was also examined in the experiments. Compared to the conventional library search method, whose time cost of the parameter extraction is concentrated on the library search itself, the interpolation-based library search method needs extra time on the multi-interpolation on the fitting errors as well as the related search operations, and the correction-based library search method needs extra time to calculate the correction term. Figure 6 depicts the time

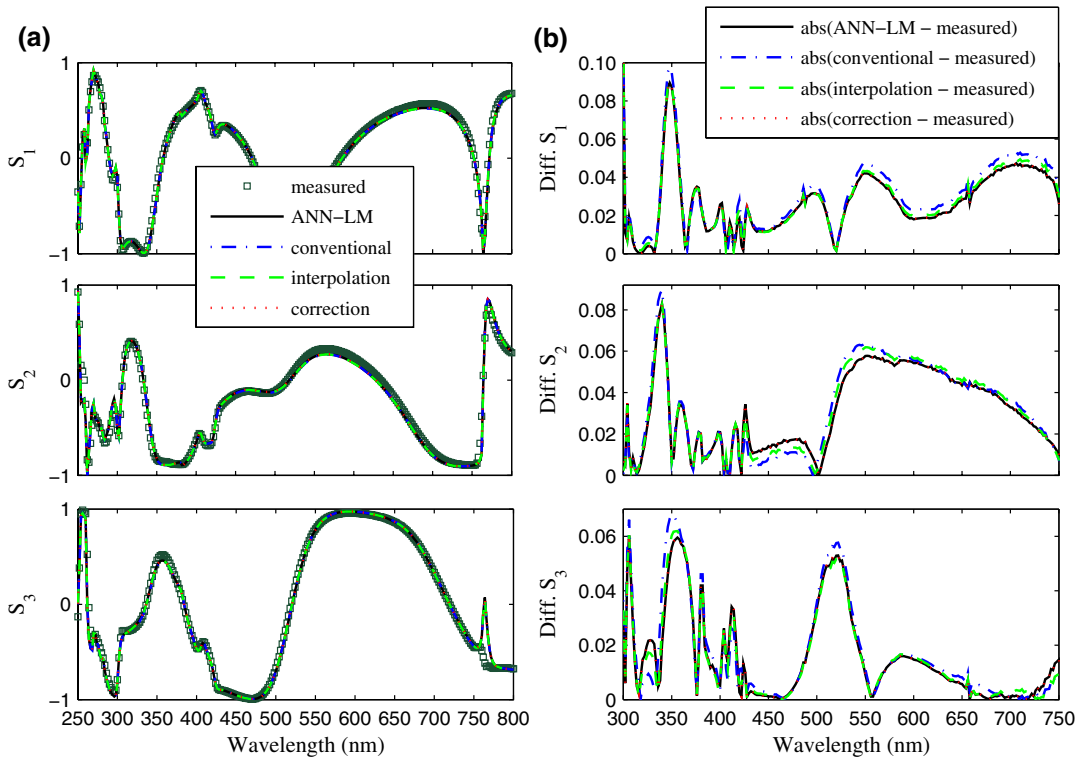

Fig. 5. (a) Measured Stokes vector elements for No. 16 die of the grating sample shown in Fig. 3 and the fitted Stokes vector elements calculated from the structural parameters presented in Table 2 extracted by the conventional library search method, the interpolation-based library search method, the correction-based library search method, and the ANN-LM combined method. (b) The absolute fitting errors between the calculated and measured Stokes vector elements.

cost for the 35 dies of the silicon wafer on a 3.64 GHz Xeon workstation (HP Z800). The mean time cost for the 35 dies is 0.534 s by the conventional library search method, 1.179 s by the interpolation-based library search method, and 0.536 s by the correction-based library search method, respectively. Figure 6 implies that the extra time spent on calculating the correction term in the correction-based library search method is less than 0.002 s, while the extra time spent on interpolating fitting errors in the interpolation-based library search method is about 0.645 s. Thus, as shown in Fig. 6, the time cost of the proposed correction-based library search method in the parameter extraction is much less than that of the interpolation-based library search method and is almost identical to that of the conventional library search method. We can therefore further conclude that the correction-based library search method has better performances than the interpolation-based library search method and can achieve a much higher measurement accuracy for a pregenerated signature library without remarkable influence on the final search speed. It is also worthwhile to point out that the high search speed characteristic of the correction-based library search method is of great importance for real-time process control in microelectronic manufacturing.

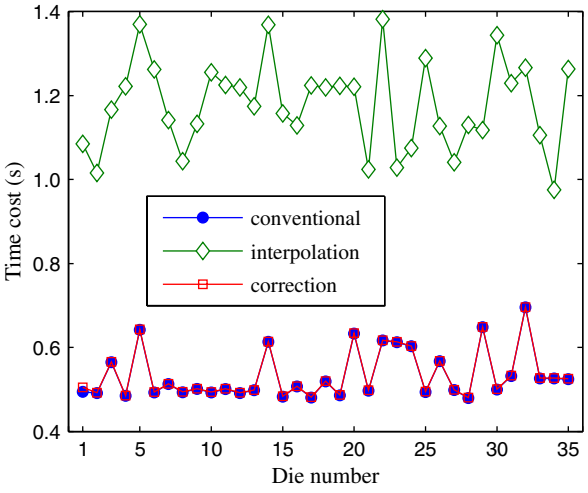

Fig. 6. Time cost of the conventional library search method, the interpolation-based library search method, and the correction-based library search method in the parameter extraction with Library 1# for the 35 dies of the investigated silicon wafer.

The proposed correction-based library search method and the interpolation-based library search method were applied to extract structural parameters from the measured signatures with Library 2# in order to further examine their performances with a smaller signature library. The conventional library search method was also applied, but with Library 1#, in order to make a comparison. The absolute errors and the corresponding mean absolute errors of the extracted structural parameters *TCD*, *SWA*, and Hgt_1 for the 35 dies of the silicon wafer are presented in Fig. 7. As shown in Figs. 4 and 7, the measurement

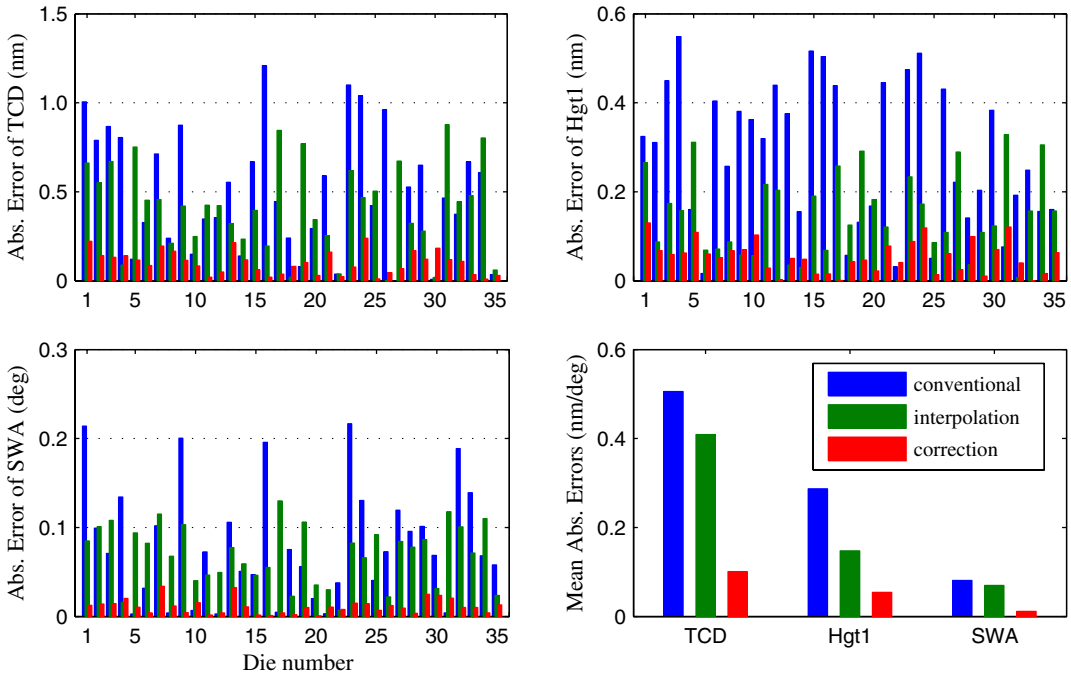

Fig. 7. Absolute errors of the structural parameters *TCD*, Hgt_1, and *SWA* obtained by the conventional library search method with Library 1#, the correction-based library search method as well as the interpolation-based library search method with Library 2#. The mean absolute errors of the extracted structural parameters for the 35 dies of the investigated silicon wafer are shown in the bottom right corner.

accuracy of the conventional library search method remains unchanged since it was applied to extract structural parameters from the same measured signatures with the same signature library (Library 1#) in the former and latter processes of parameter extraction. As can be observed from Fig. 7, the final measurement accuracy is still improved by using the correction-based library search method and the interpolation-based library search method even with a smaller signature library. A comparison between Figs. 4 and 7 also reveals that the measurement accuracy of both the correction-based library search method and the interpolation-based library search method decreases with the increase of the grid interval of the library. This is because the grid interval is closely related to the accuracy of the calculation of the correction term in the correction-based library search method and the accuracy of the multi-interpolation on the fitting errors in the interpolation-based library search method. With the increase of the grid interval of the library, the accuracy of the calculation of the correction term and the multi-interpolation on the fitting errors will decrease. However, we can observe from Fig. 7 that the accuracy of the proposed correction-based library search method is still much higher than that of the interpolation-based library search method. It might be because the gradient-based correction term in the correction-based library search method is much more accurate than the interpolation on fitting errors in the interpolation-based library search method, especially if the grid interval of the library is sparse. It is also noted from Fig. 7 that the correction-based library search method with a smaller signature library (i.e., Library 2#) can still achieve much higher measurement accuracy than the conventional library search method with a larger signature library (i.e., Library 1#) does. It implies that we can use the correction-based library search method to achieve the required measurement accuracy with a much smaller signature library. Thus the burden of library construction can be greatly relieved.

In this section, the validity of the proposed correction-based library search method was examined in detail through experiments performed on a photoresist grating sample with a pitch of 400 nm and nominal critical dimension of 200 nm. Compared with today's technology node, the values of the critical dimension and pitch of the investigated grating sample may seem too large. In addition, the number of floating parameters and the scale of the signature libraries in the process of parameter extraction may seem fairly small. It is worth pointing out that the correction-based library search is sample independent and can be easily extended without any change to more complex nanostructures with more undetermined structural parameters. Because the number of floating measurands M is always less than the number of spectral points N, the time complexity in calculating the correction term given by Eq. (11) will be always less than $O(N^3)$, which is ignorable even when the number of floating measurands increase. One issue that needs to be discussed is the time cost in obtaining the searched solution $\mathbf{x}_s$ of the inverse problem in the first step of the correction-based library search method when the library contains millions of signatures. Obviously, the time cost in obtaining the searched solution $\mathbf{x}_s$ will take longer

when the scale of the signature library becomes larger. Several library search algorithms have been reported with an emphasis on the speed and accuracy of the matching result in the past decades [21–23]. Detailed description of these algorithms is beyond the scope of this paper, one can consult the corresponding references for more details. Anyway, it is expected that the proposed correction-based library search method will provide a useful and practical means for solving the inverse problem in state-of-the-art optical scatterometry.

4. Conclusions

In this paper, a correction-based library search is proposed to improve the measurement accuracy in optical scatterometry. Experiments performed on a photoresist grating sample have demonstrated that the proposed correction-based library search method can be applied to solve the inverse problem with much higher accuracy than the conventional library search method and the interpolation-based library search method. As the computational penalty of the error estimation is negligible, and no interpolation is introduced, the efficiency of the correction-based library search method is as high as the conventional library search method. The experimental results also show that the proposed method can achieve a more accurate measurement even with a smaller signature library than the conventional library search method with a larger signature library. The significant improvement in accuracy enables us to achieve more accurate measurements and less time consumption at the same time by applying the correction-based library search method with a small signature library.

This work was funded by the National Natural Science Foundation of China (Grant Nos. 91023032, 51005091, and 51121002) and the National Instrument Development Specific Project of China (Grant No. 2011YQ160002).

References

1. B. K. Minhas, S. A. Coulombe, S. Sohail, H. Naqvi, and J. R. McNeil, "Ellipsometric scatterometry for metrology of sub-0.1 μm linewidth structures," Appl. Opt. **37**, 5112–5115 (1998).
2. H. T. Huang, W. Kong, and F. L. Terry, "Normal-incidence spectroscopic ellipsometry for critical dimension monitoring," Appl. Phys. Lett. **78**, 2985–3983 (2001).
3. C. H. Ko and Y. S. Ku, "Overlay measurement using angular scatterometer for the capability of integrated metrology," Opt. Express **14**, 6001–6010 (2006).
4. T. Novikova, A. De Martino, S. B. Hatit, and B. Drévillon, "Application of Mueller polarimetry in conical diffraction for critical dimension measurements in microelectronics," Appl. Opt. **45**, 3688–3697 (2006).
5. H. J. Patrick, R. Attota, B. M. Barnes, T. A. Germer, R. G. Dixson, M. T. Stocker, R. M. Silver, and M. R. Bishop, "Optical critical dimension measurement of silicon grating targets using focal plane scatterfield microscopy," J. Micro/Nanolith. MEMS MOEMS **7**, 013012 (2008).
6. J. Li, J. J. Hwu, Y. Liu, S. Rabello, Z. Liu, and J. Hu, "Mueller matrix measurement of asymmetric gratings," J. Micro/Nanolith. MEMS MOEMS **9**, 041305 (2010).
7. M. G. Moharam, E. B. Grann, D. A. Pommet, and T. K. Gaylord, "Formulation of stable and efficient implementation of the rigorous coupled wave analysis of binary gratings," J. Opt. Soc. Am. A **12**, 1068–1076 (1995).
8. L. Li, "Use of Fourier series in the analysis of discontinuous periodic structures," J. Opt. Soc. Am. A **13**, 1870–1876 (1996).
9. S. Y. Liu, Y. Ma, X. G. Chen, and C. W. Zhang, "Estimation of the convergence order of rigorous coupled-wave analysis for binary gratings in optical critical dimension metrology," Opt. Eng. **51**, 081504 (2012).
10. H. Gross, R. Model, M. Bär, M. Wurm, B. Bodermann, and A. Rathsfeld, "Mathematical modelling of indirect measurements in scatterometry," Measurement **39**, 782–794 (2006).
11. J. Pomplun and F. Schmidt, "Accelerated a posterior error estimation for the reduced basis method with application to 3D electromagnetic scattering problems," SIAM J. Sci. Comput. **32**, 498–520 (2010).
12. Y. Nakata and M. Kashiba, "Boundary-element analysis of plane-wave diffraction from groove-type dielectric and metallic gratings," J. Opt. Soc. Am. A **7**, 1494–1502 (1990).
13. H. Ichikawa, "Electromagnetic analysis of diffraction gratings by the finite-difference time-domain method," J. Opt. Soc. Am. A **15**, 152–157 (1998).
14. E. Drége, J. Reed, and D. Byrne, "Linearized inversion of scatterometric data to obtain surface profile information," Opt. Eng. **41**, 225–236 (2002).
15. C. W. Zhang, S. Y. Liu, T. L. Shi, and Z. R. Tang, "Improved model-based infrared reflectrometry for measuring deep trench structures," J. Opt. Soc. Am. A **26**, 2327–2335 (2009).
16. C. J. Raymond, "Scatterometry for semiconductor metrology," in *Handbook of Silicon Semiconductor Metrology*, A. C. Diebold, ed. (Academic, 2001), Chap. 18, pp. 477–514.
17. X. Niu, N. Jakatdar, J. Bao, and C. J. Spanos, "Specular spectroscopic scatterometry," IEEE Trans. Semicond. Manuf. **14**, 97–111 (2001).
18. C. J. Raymond, M. Littau, A. Chuprin, and S. Ward, "Comparison of solutions to the scatterometry inverse problems," Proc. SPIE **5375**, 564–575 (2004).
19. P. Thony, D. Herisson, D. Henry, E. Severgnini, and M. Vasconi, "Review of CD measurement and scatterometry," AIP Conf. Proc. **683**, 381–388 (2003).
20. C. Raymond, "Overview of scatterometry applications in high volume silicon manufacturing," AIP Conf. Proc. **788**, 394–402 (2005).
21. J. L. Bentley, "Multidimensional binary search trees used for associative searching," Commun. ACM **18**, 509–517 (1975).
22. D. T. Lee and C. K. Wong, "Worst-case analysis for region and partial region searches in multidimensional binary search trees and balanced quad trees," Acta Inform. **9**, 23–29 (1977).
23. A. Gionis, P. Indyk, and P. Motwani, "Similarity search in high dimensions via hashing," Proc. VLDB, 518–529 (1999).
24. Y. S. Ku, S. C. Wang, D. M. Shyu, and N. Smith, "Scatterometry-based metrology with feature region signatures matching," Opt. Express **14**, 8482–8491 (2006).
25. M. Littau, D. Forman, J. Bruce, C. J. Raymond, and S. G. Hummel, "Diffraction signature analysis methods for improving scatterometry precision," Proc. SPIE **6152**, 615236 (2006).
26. X. G. Chen, S. Y. Liu, C. W. Zhang, and J. L. Zhu, "Improved measurement accuracy in optical scatterometry using fitting error interpolation based library search," Measurement **46**, 2638–2646 (2013).
27. T. A. Germer, H. J. Patrick, R. M. Silver, and B. Bunday, "Developing an uncertainty analysis for optical scatterometry," Proc. SPIE **7272**, 72720T (2009).
28. N. F. Zhang, R. M. Silver, H. Zhou, and B. M. Barnes, "Improving optical measurement uncertainty with combined multitool metrology using a Bayesian approach," Appl. Opt. **51**, 6196–6206 (2012).
29. C. M. Herzinger, B. Johs, W. A. McGahan, J. A. Woollam, and W. Paulson, "Ellipsometric determination of optical constants for silicon and thermally grown silicon dioxide via a multi-sample, multi-wavelength, multi-angle investigation," J. Appl. Phys. **83**, 3323–3336 (1998).
30. G. E. Jellison, Jr. and F. A. Modine, "Parameterization of the optical functions of amorphous materials in the interband region," Appl. Phys. Lett. **69**, 371–373 (1996).